Low-energy-electron-diffraction system using a high-performance electron gun and position-sensitive detectors

F.-K. Men, B. L. Clothier,[a] and J. L. Erskine
Department of Physics, University of Texas at Austin, Austin, Texas 78712

(Received 5 November 1992; accepted for publication 1 March 1993)

A new low-energy-electron-diffraction (LEED) instrument is described that combines resistive-anode-based position-sensitive detectors with a high-resolution electron gun capable of producing a beam having high spatial coherence (large instrument transfer width). The system produces digitized images of LEED patterns as well as high-resolution spot profiles of individual beams using incident currents in the picoampere range, thus vastly reducing or eliminating electron beam damage to sensitive surfaces. The display resolution of both spot profile and full display images is 1024×1024 channels, and the dynamic range is 16 bits ($\approx10^4$) per channel. The resistive anode pulse processing electronics limits maximum data acquisition rates to 1×10^6 s^{-1}. Specially developed software permits manipulation and numerical processing of the digitized two-dimensional images at full resolution to produce spot contour maps, spot line profiles along arbitrary directions, Fourier transforms of spot profiles, integrated spot intensities, and intensity vs voltage curves with suitably subtracted background.

I. INTRODUCTION

Low-energy electron diffraction (LEED) is a well-established and versatile technique for characterizing surface structure.[1–5] Commercial display-type LEED instruments consisting of an electron gun, retarding grids, and a fluorescent screen permit direct viewing of the diffraction pattern produced by a crystal surface. The LEED pattern characterizes the two-dimensional symmetry of the surface crystal lattice. The diffracted intensities change with electron gun energy, and careful measurements of the intensity vs acceleration voltage, generally referred to as $I(V)$ curves, permit detailed structural analysis based on multiple scattering formalisms that are now highly developed.[1–3] New personal computer (PC) compatible solid-state camera technology, new spatially sensitive detectors, and sophisticated image processing technology permit a convenient means of digitally recording display LEED patterns and for performing $I(V)$ measurements.

The shape of LEED spots and the angle-dependent background also contain structural information about the surface.[6,7] In order to obtain the maximum benefit from detailed analysis of LEED spot profiles, it is necessary to have an electron diffractometer with a response function that approaches the ideal limit (corresponding to diffraction of a plane wave) so that the measured spot profile is characteristic of the surface structure rather than the instrument response function or a convolution of both of these functions. The required technology for spot profile LEED studies has been developed in several laboratories,[4,5] and many important applications have been described in the literature. In addition, good commercial spot profile LEED instruments have been available in the past,[8] and apparently are again becoming available.[9]

In the past, special requirements have resulted in novel LEED system designs that utilized channel plates to amplify diffracted beam intensities.[10–12] These instruments, which utilized both fluorescent screen detectors[10] and resistive anode technology,[11,12] permit LEED analysis of electron beam sensitive systems such as ordered structures of rare gas atoms physisorbed on a surface and unstable chemisorbed species. New applications requiring similar conditions (very low electron beam intensity) include the new high-T_c superconductor surfaces which appear to be unstable under electron beams.

The commercial availability of high-resolution resistive-anode-based position-sensitive detectors[13] now permits configuring versatile electron diffraction systems that combine the benefits of a high-angular resolution gun suitable for spot profile analysis, and a low-current full-display instrument suitable for intensity analysis of delicate surfaces. The present paper describes such an instrument.

II. INSTRUMENTATION

The principal components of our new LEED instrument are described in three subsections covering the high-resolution electron gun, the resistive-anode detectors, and the data manipulation software. The vacuum system that incorporates the LEED instrumentation utilizes standard ultrahigh vacuum system components, but with special attention to specific requirements of precision electron diffraction measurements. Based on our past experience with low-energy electron spectroscopy, a μ-metal chamber was judged to be cost effective in eliminating distortion of electron trajectories by stray magnetic fields while minimizing the pumped surface area. In addition, special attention was given to minimizing mechanical vibrational resonances. Both high-resolution LEED and scanning tunneling microscopy (an anticipated addition to the system) require good mechanical stability. The 400 ℓ/s ion pump is isolated from the chamber by an 8-in.-diam gate valve permitting it to remain on when venting the system or admitting gas

[a]Present address: United States Air Force Academy, Colorado Springs, Colorado.

 © 1993 American Institute of Physics

Downloaded 14 Oct 2009 to 128.83.114.33. Redistribution subject to AIP license or copyright; see http://rsi.aip.org/rsi/copyright.jsp

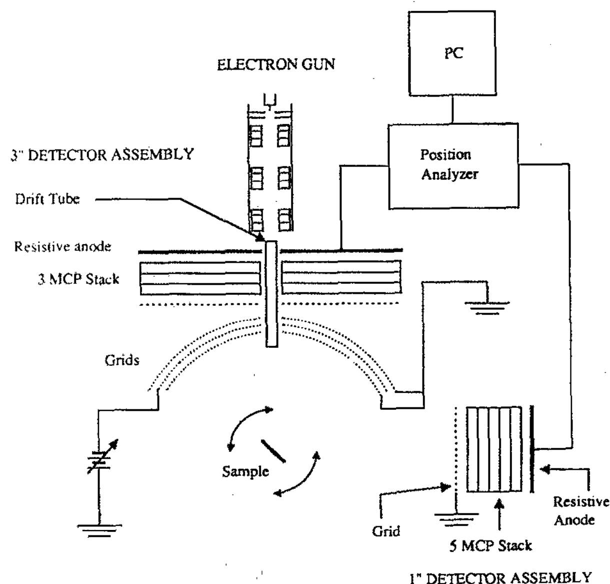

FIG. 1. LEED system block diagram. The high-performance electron gun is located behind the 3 in. detector and centered along the drift tube axis. A grid system is placed in front of the 3 in. detector to provide field free regions, and a uniform retarding field along electron trajectories. A high spatial-resolution 1-in.-diam detector is placed at a position 8.5 in. away from sample with its surface normal perpendicular to the incident beam. The sample is mounted on a rotatable *xyz* manipulator. The position of an event is calculated in an analog mode and then converted into digital signal by the position analyzer. The digitized images are transferred to a PC for data processing.

doses during experiments. The valve was also found very useful for eliminating background counts in the large microchannel plate detector that result from stray high-energy charged particles produced in the pump. A large-capacity liquid-nitrogen-cooled titanium sublimation pump maintains low pressures during data acquisition in experiments where low background counting rates require that the ion pump be valved closed. The chamber base pressure is maintained in the low 10^{-11} Torr range. The μ-metal chamber provides ports for the LEED components as well as for other bolt-on analysis capabilities including Auger spectroscopy.

Figure 1 presents a schematic diagram of the LEED system components consisting of a high-resolution electron gun, which is mounted on an acuport/*xy* stage combination for precise positioning, and two microchannel plate (MCP)/resistive anode detectors, one having a 3 in. effective diameter, the other a 1 in. effective diameter. The 3-in.-diam detector assembly has a 6 mm hole in the center to accommodate the electron drift tube as shown in the figure. Both detector systems are serviced by the same preamp position analyzer and computer.[13]

A. High-resolution gun

Our high-resolution electron gun is based on a design reported by Cao and Conrad.[14] The mechanical details of our gun are shown in Fig. 2. A complete description of the gun mechanical design, assembly alignment jigs, control electronics, and initial tests is available.[15] Table I summarizes critical dimensions. The gun consists of an indirectly

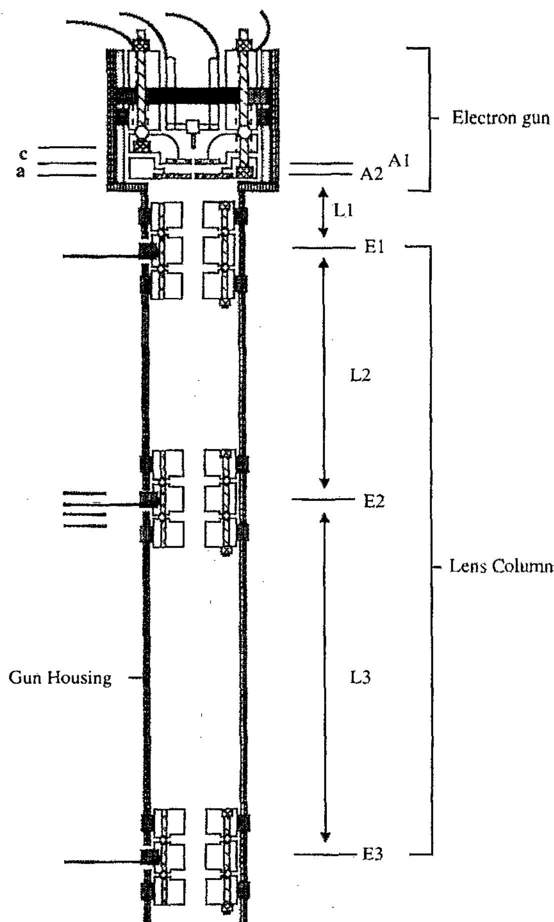

FIG. 2. Schematic drawing of the electron gun. The LaB_6 cathode is positioned on the electron optical axis by three adjustment screws, prior to sliding the entire electron gun into the gun housing. The cathode-to-aperture A_1 distance c is 0.048 in. The distance a between apertures A_1 and A_2 is 0.046 in. E_1, E_2, and E_3 are the three Einzel lenses mentioned in the text. The distances L_1, L_2, and L_3 between the centers of those Einzel lens elements are 0.281, 1.276, and 2.268 in., respectively. E_2 has four electrical leads due to it being a steering lens. Critical dimensions and distances are summarized in Table I.

heated LaB_6 filament[16] and two beam defining apertures A_1 and A_2, followed by a lens column having three Einzel lenses, E_1, E_2, and E_3. The filament assembly, including apertures A_1 and A_2, can be removed as a unit. This permits convenient alignment of the LaB_6 tip while viewed through A_1 and A_2 using a microscope. The modular design also permits exchanging the LaB_6 assembly with a field emission tip assembly if higher source brightness becomes necessary. Based on performance achieved to date, a field emission tip will not be required to achieve instrument transfer widths of 2000 Å (the transfer width is defined and discussed in Sec. III).

Our present gun utilizes aperture diameters $A_1 = A_2 = 0.020$ in., and achieves a transfer width exceeding 800 Å at 100 eV beam energy with the filament operating far below maximum emission. Under these conditions, the

Downloaded 14 Oct 2009 to 128.83.114.33. Redistribution subject to AIP license or copyright; see http://rsi.aip.org/rsi/copyright.jsp

TABLE I. Electron gun critical dimensions.[a]

c	0.048 in.
a	0.046 in.
A_1	0.020 in. aperture diameter and thickness
A_2	0.020 in. aperture diameter and thickness
L_1	0.281 in.
L_2	1.276 in.
L_3	2.268 in.

[a] c: Distance between cathode and aperture A_1, a: Distance between apertures A_1 and A_2, L_1: Distance between aperture A_2 and lens E_1, L_2: Distance between lenses E_1 and E_2, L_3: Distance between lenses E_2 and E_3.

beam current is several nanoamps, which is sufficient to operate the detectors near their maximum counting rate of $10^6\ s^{-1}$.

In our gun design, E_2 consists of four cylindrical quadrants which permit steering of the beam. Our application requires the gun to produce a beam precisely along the gun housing axis so that it can pass through the center of the drift tube (refer to Fig. 1). The steering capability at E_2 permits compensation for very small misalignments in E_1 or in the position of the filament assembly. We have found, however, that the centering jigs[15] used in mechanically aligning the lens column and electron gun produce very good axial alignment: the asymmetry of steering voltages at E_2 is generally near zero.

The gun housing is mounted on a track system which allows adjustment of the gun to sample distance over the range of a few inches.

B. Detectors

Two commercially available[13] resistive-anode-based image detectors are used in our LEED system. The display LEED detector consists of a set of three hemispherical grids[17] followed by a planar field terminating screen and the MCP stack/resistive anode detector. The center hemispherical grid is operated at a negative potential just below the gun acceleration voltage to repel secondary electrons, and the remaining two hemispherical grids and the planer screen are grounded to provide field free regions that preserve the initial electron trajectories. The first MCP is operated at about 50 eV above the gun acceleration voltage. The display LEED detector utilizes a stack of 3 MCPs. This stack provides sufficient gain to permit using the same preamplifier/position computer electronics for both the 1-in.-diam detector (which utilizes a 5 MCP stack) and the 3-in.-diam detector. The quoted spatial resolution of the three inch detector is ≈ 100 lines/in. or a total of ≈ 300 lines across the detector face. The 1 in. detector spatial resolution is 800 lines/in.

The presence of a 6 mm hole in the MCPs and resistive anode does not appear to substantially affect the accuracy of the position sensitive detection. However, we discovered an undesirable effect when a grounded drift tube was first tried in the system. This introduced a circular region of reduced response around the hole. To better understand

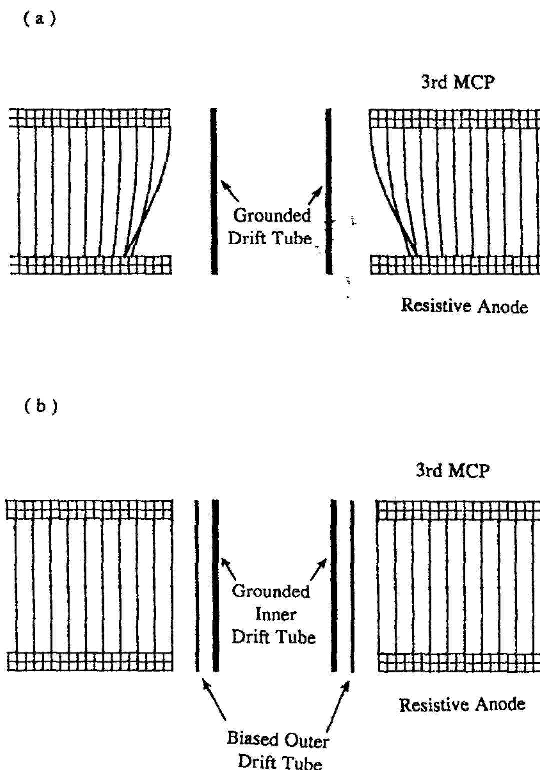

FIG. 3. Schematic diagram of two drift tube designs and the corresponding electric field distributions obtained from computer analysis for the two configurations. In (a), the drift tube is at ground potential. We can see the electric field lines are repelled by the drift tube. After inserting an insulating spacer between the inner and outer drift tube and with outer drift tube being biased close to the resistive anode potential, we correct the field-line bending problem, as shown in (b). For both configurations, the third MCP and resistive anode are at 2720 and 2920 V, respectively. The outer drift tube in (b) is set to 2820 V.

this effect, we carried out electron ray-tracing simulations[18] of the 3 in. detector in the region between the third MCP and the resistive anode. Typical results are illustrated in Fig. 3 along with two drift tube designs. The simulations suggested that operation of the MCP-resistive anode combination is optimized when the potential of the drift tube is between the potentials of the last MCP and the resistive anode, as shown in Fig. 3(b). The solution to this problem is to incorporate an insulating spacer between the inner and outer surfaces of the drift tube. This permits the inner surface to be operated at ground potential and the outer surface to be operated near the anode potential. With this modified drift tube, the 3 in. detector yields nearly distortion-free performance over the entire active area.

For spot profile analysis, a high spatial resolution 1-in.-diam MCP/resistive anode detector is used. The total path distance from the electron gun apertures to the detector face is approximately 20 in. and the 1 in. detector achieves a spatial resolution of 800 lines/in. The ultimate angular resolving power of the detection system is therefore approximately 6×10^{-5} rad (0.06 mrad). The grid placed in front of the 1 in. position-sensitive detector is a 55% transmission Cu mesh having 750 lines/in.,[19] so the actual detector resolving power is slightly lower.

Downloaded 14 Oct 2009 to 128.83.114.33. Redistribution subject to AIP license or copyright; see http://rsi.aip.org/rsi/copyright.jsp

C. Computer software

The position sensitive detector creates a digitized image (a frame) having spatial resolution of 1024×1024 and dynamic range of 16 bits (or $\approx10^4$ counts full scale). Our first requirement was to perform simple manipulation of these frames (addition, subtraction, storage, retrieval) without a loss in resolution. We were unable to find a commercially available PC compatible software package that meets this requirement. Existing software, and all popular PC-based image processors are limited by the hardware they are designed to support and control: the SVGA-class of images characterized by 1024×768 pixels, with 8-bit dynamic range (256 counts).

We have developed PC software that meets the following requirements: it directly manipulates the $1024\times1024\times16$-bit frames, and at the same time, represents the results using the SVGA-class display format. In other words, all displayed images are based on the SVGA-class format, but all tasks performed (frame averaging, background subtraction, integrated intensities, spot profile cuts, etc.) are performed at full frame resolution (i.e., the raw data rather than the on-screen image).

Our software package is written using Borland's Tubo C++ development system, and presently it is being ported to a 32-bit version using IBM's *C* Developer's Workset for OS/2 2.0.

III. PERFORMANCE

We first address some of the technical issues required to specify the performance of a spot profile LEED system, i.e., the instrument transfer width that specifies the resolving power. The measured beam intensity $I_m(k)$ is the convolution of the actual intensity function $I(k)$ which is the intensity one would measure with a perfect instrument, and the instrument response function, $T(k)$, which represents the instrument response to a diffracted beam from a perfectly ordered, rigid surface. From the convolution theorem, we have

$$F\{I_m(k)\}=F\{I(k)*T(k)\}=i(r)t(r),$$

where $i(r)=F\{I(k)\}$ is the autocorrelation function and $t(r)$ the Fourier transform of $T(k)$.

In order to extract information correlating individual surface scatterers from the autocorrelation function, $t(r)$ cannot be zero everywhere. Park *et al.*[20] define the transfer width of an instrument as the full width at half-maximum (FWHM) of $t(r)$, assuming Gaussians for all functions. The transfer width is frequently, although incorrectly, interpreted as the maximum distance between two scatterers over which the instrument can still detect the phases of the scatterers as being correlated.[21]

The upper panel of Fig. 4 shows the LEED image of a Si(100)-2×1 surface taken by the 3 in. detector. The central dark area is produced by a 0.4-in.-diam mask placed in front of the detector for testing purposes. To emphasize the diffuse scattering distribution, we choose to use a 1-to-1 count to gray scale ratio from 0 to 63, the maximum gray scale range of our PC; that means, a zero count corresponds to black, and a count equal to or greater than 63 is white in the image. The brightest spot, the (00) beam located at the lower center left, has a peak intensity of 1983 counts. The (10) spot, second brightest spot, has a peak count of 598. As can be seen from the image, the diffuse scattering distribution is rather uniform across the entire detector plane and quite low. In this image, the ratio of the maximum count to diffuse scattering is less than 1%. In order to display the (00) spot, the sample has been tilted away from normal incidence position. Therefore, equivalent spot intensities are not equal. The grid-type structure in the image is due to the Moire interference effects of the three hemispherical grids.[22] This image took 480 s to acquire. The incident beam energy and current are 120 eV and 0.3 pA, respectively.

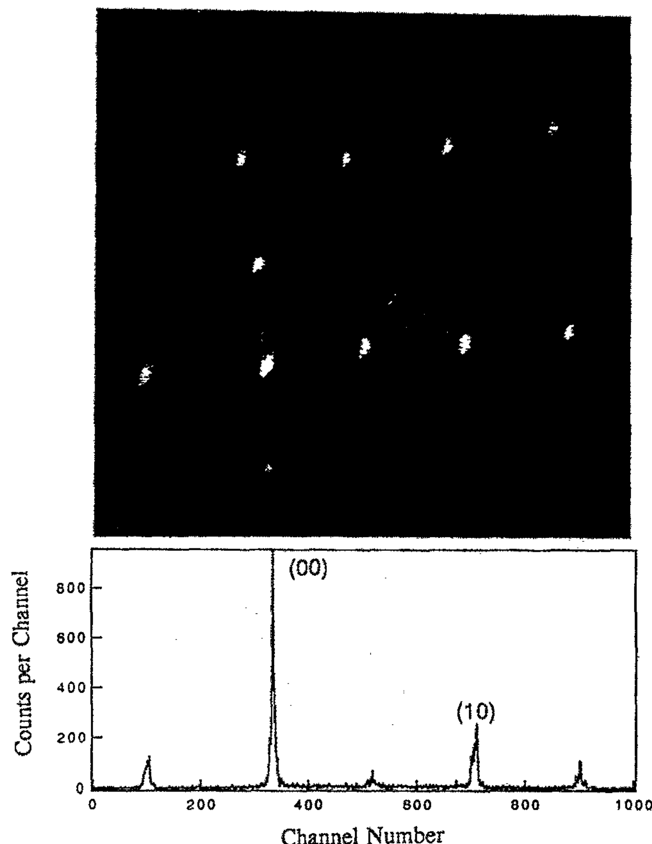

FIG. 4. LEED image of Si(100)-2×1 surface. Image is taken by the 3 in. detector. The central dark region is the image of a 0.4-in.-diam disk placed in front of the detector. (00) spot is located at lower central left with a peak count of 1983. The peak count to diffuse scattering ratio is less than 1%. The grid-type structure is the result of Moire interference pattern produced by the hemispherical grids. Incident beam energy is 120 eV. Data acquisition time is 480 s. Bottom plot shows the intensity profile by cutting along the [10] direction. We were not able to make cuts right through peak positions due to diffracted spots not lining up perfectly.

The lower panel of Fig. 4 shows the intensity profile resulting from a one-dimensional cut along the [10] direction. Because of the off-normal incidence and the use of a planar detector, the diffracted spots do not line up perfectly in the image. In order to show as many spots as possible, we were unable to make cuts through the spot peak positions.

Downloaded 14 Oct 2009 to 128.83.114.33. Redistribution subject to AIP license or copyright; see http://rsi.aip.org/rsi/copyright.jsp

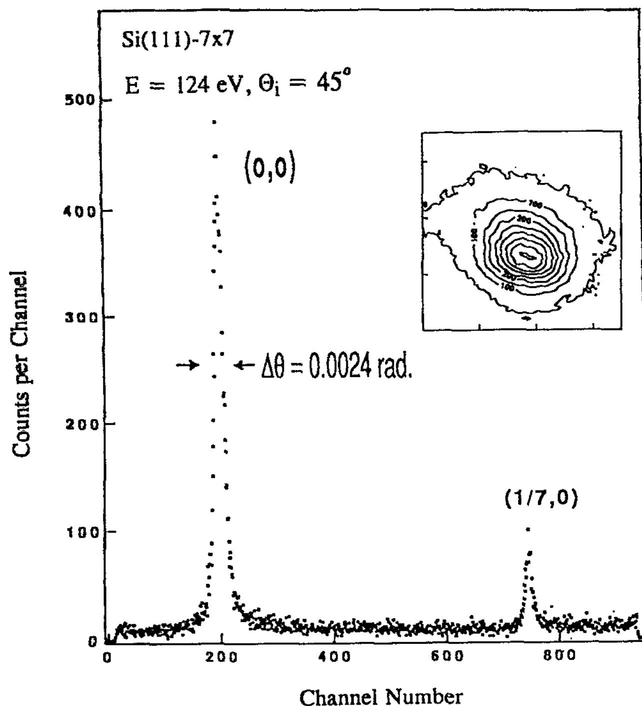

FIG. 5. Spot profile of Si(111)-7×7 surface. The line profile was made by cutting a digitized LEED image taken by the 1-in.-high spatial-resolution resistive anode detector along a principle axis. Shown are (00) and (1/7,0) spots. The FWHM of (00) spot is 0.0024 rad. By assuming the surface is perfectly flat and periodic, the transfer width of the LEED system is no less than 650 Å. Incident angle and beam energy are 45° and 124 eV, respectively. Data acquisition time is 202 s. Insert is a contour plot of the (00) spot.

The integrated spot intensity can readily be extracted from the image by summing over all channels within a defined region of interest surrounding the spot for counts above the diffuse scattering background. By doing so, we can make *I-V* plots for various spots simultaneously.

The ability to collect a major portion of the diffuse scattering background permits this LEED system to measure the diffuse LEED intensities for disordered adsorbates.[7] By using numerical differentiation technique, display-type Auger electron emission patterns can also be obtained. Forward scattering analysis of these patterns also provides a surface structure probe.

Figure 5 displays a line profile cut from an image taken by the 1 in. detector. The beam incident angle is 45°, and the detector surface normal is perpendicular to the incident beam direction, as shown in Fig. 1. Shown in the figure are the (00) and (1/7,0) spots of a precisely cut Si(111)-7×7 surface. The specified alignment accuracy of this surface should yield a terrace width of $\approx$1000 Å. The FWHM of the (00) spot is 0.0024 rad. By assuming the surface is perfectly flat and periodic, and that the entire spot width is due to the instrumental broadening, we can set a conservative lower bound of the transfer width of this LEED system to be 650 Å. By simply reducing the aperture sizes of A_1 and A_2, we believe this value can be further increased. (The filament maximum current is still far greater than needed to provide the saturation current at the detector.) The Fig. 5 insert is a contour plot of the (00) spot. Such plots can be used to study, e.g., the elongation of beam profiles during thin film growth.[23] The image took 202 s to acquire. The incident beam energy is 124 eV.

ACKNOWLEDGMENTS

We would like to thank Ivan Salazar for developing data processing software, and Peter Stair, Sam Fain, and Ron Malic for useful discussions. We also thank Dr. P. Wagner, Wacker Chemitronic, Burghausen, Germany for supplying us with high-quality, well-oriented Si wafers for this work. This work is partly supported by the Science and Technology Center at The University of Texas at Austin under Grant No. CHE-8920120, and by the R. L. Welch Foundation Grant No. F-1015. The instrumentation reported here was obtained through a NSF instrument Grant No. DMR-9003179.

[1] J. B. Pendry, *Low Energy Electron Diffraction* (Academic, New York, 1974).
[2] M. A. Van Hove and S. Y. Tong, *Surface Crystallography by LEED* (Springer, Berlin, 1979).
[3] M. A. Van Hove, W. H. Weinberg, and C.-M. Chan, *Low-Energy Electron Diffraction* (Springer, Berlin, 1986).
[4] M. Henzler, in *Electron Spectroscopy for Surface Analysis*, edited by H. Ibach (Springer, Berlin, 1977).
[5] M. G. Lagally and J. A. Martin, Rev. Sci. Instrum. **54**, 1273 (1983).
[6] D. W. Kruger, D. E. Savage, and M. G. Lagally, Phys. Rev. Lett. **63**, 402 (1989).
[7] J. B. Pendry, in *The Structure of Surfaces*, edited by M. A. Van Hove and S. Y. Tong (Springer, Berlin, 1985).
[8] Leybold Inc., SPA LEED, Export, PA.
[9] Omicron Associates, Spot Profile Analysis LEED, Pittsburgh, PA.
[10] M. D. Chinn and S. C. Fain, J. Vac. Sci. Technol. **14** 314 (1977).
[11] P. C. Stair, Rev. Sci. Instrum. **51**, 132 (1980).
[12] E. G. McRae, R. A. Malic, and D. A. Kapilow, Rev. Sci. Instrum. **56**, 2077 (1985).
[13] Two resistive anode detectors and position-sensing electronics are supplied by Quantar Technology Inc., Santa Cruz, CA.
[14] Y. Cao and E. H. Conrad, Rev. Sci. Instrum. **60**, 2642 (1989).
[15] B. L. Clothier, M. A. Thesis, University of Texas, 1991.
[16] Kimball Physics Inc., model ES-423B, Wilton, NH.
[17] Perkin-Elmer Inc., Eden Prairie, MN.
[18] A software package SIMION is used for the simulations. SIMION is written by D. A. Dahl and J. E. Delmore at the Idaho National Engineering Laboratory, Idaho.
[19] Buckbee-Mears Operation, St. Paul, MN.
[20] R. L. Park, J. E. Houston, and D. G. Schreiner, Rev. Sci. Instrum. **42**, 60 (1971).
[21] For a more detailed discussion about transfer width, please see G. Comsa, Surf. Sci. **81**, 57 (1979).
[22] To resolve the problem associated with the Moire effect, we can either use hemispherical grids with higher mesh density or remove the entire grid system. The retarding fields can be supplied by biasing the first MCP when the grid system is removed. Our current grid system has a mesh density of 100 lines per inch with 83% transmission.
[23] G. S. Glander and M. B. Webb, Surf. Sci. **224**, 60 (1989).

Downloaded 14 Oct 2009 to 128.83.114.33. Redistribution subject to AIP license or copyright; see http://rsi.aip.org/rsi/copyright.jsp